Advances in Science and Technology Research Journal

*Advances in Science and Technology Research Journal* 2024, 18(5), 332–341
https://doi.org/10.12913/22998624/190548
ISSN 2299-8624, License CC-BY 4.0

Received: 2024.04.15
Accepted: 2024.07.20
Published: 2024.08.01

# Investigation of Hot-Dip Galvanising Influence on the Buckling Resistance of Steel Angles

Marcin Górecki[1*], Kamil Jastrzębski[2], Lucjan Ślęczka[3]

[1] Faculty of Civil Engineering and Architecture, Lublin University of Technology, ul. Nadbystrzycka 40, 20-618 Lublin, Poland

[2] Doctoral School of the Rzeszów University of Technology, al. Powstańców Warszawy 12, 35-959 Rzeszów, Poland

[3] Faculty of Civil and Environmental Engineering and Architecture, Rzeszów University of Technology, ul. Poznańska 2, 35-084 Rzeszów, Poland

* Corresponding author's e-mail: m.gorecki@pollub.pl

## ABSTRACT

The buckling curves, which enable the prediction of buckling resistance of steel structural elements, are physically connected with their type of cross-section, initial out-of-straightness, and the magnitude of residual stresses due to the different manufacturing technologies. It is known that hot-dip galvanisation changes and relives residual stresses, but so far the current design provisions do not take directly into account the impact of hot-dip galvanising on the reduction of residual stresses, and thus the reduction the generalised imperfection in the Ayrton-Perry model. The paper presents the difference between the relative buckling resistance of steel angles with residual stresses resulting from hot rolling and the same elements in which the magnitude of residual stresses was decreased by the hot-dip galvanising process. Carried out tests and geometrically and materially non-linear analyses with imperfections (GMNIA) have shown that angles with residual stresses reduced by heat treatment caused by hot-dip galvanising have higher buckling resistance compared to those with residual stresses after hot rolling. This increase ranges from 2 to 7%. The analyses carried out confirmed that the predicted reduction factors $\chi$ exhibit values closer to the buckling curve 'a', but these values do not reach the '$a_0$' curve recommended by the EN 50341-1 standard.

**Keywords:** hot-dip galvanising, buckling resistance, residual stresses, GMNIA analysis.

## INTRODUCTION

Steel lattice towers are one of the most frequently built structures in Europe and throughout the world. They are usually used for telecommunication and power transmission purposes. They are made of individual elements, manufactured in the workshop, and assembled at the construction site to form a self-supporting cantilevered space truss with a triangular, square, or rectangular plan. Individual elements joined by bolted connections form legs and bracing elements, which are very frequently made from equal leg angle sections. As discussed by Vayas et al. [1], this type of section provides easy connections, resulting in a simpler assembly. Furthermore, appropriate long-life corrosion protection is ensured, since all angle sizes are fully amenable to hot-dip galvanising, in contrast to several other types of open and closed sections. As the shaft of tower is a space truss, the considered ultimate limit states requirements are checked in leg and bracing members as resistance of cross-sections in tension or their buckling resistance in compression. In the case of slender elements used in towers, the buckling resistance is a crucial limit state.

The design buckling procedure in modern design standards [2] is based on the Ayrton-Perry generalised imperfection model, taking into account in one equivalent imperfection such influences as variations in cross-sectional dimensions, initial out-of-straightness, eccentricities in load transfer, material inhomogeneities, and presence of residual stresses. Systematic theoretical and experimental research carried out in the past century [3] underscored the greatest influence of geometric imperfections and residual stresses on the resistance to buckling of compressed elements. Jan Augustyn's research [4] was one of the first to correctly indicate the influence of residual welding stresses on the buckling resistance of compression elements. Currently, the fact that residual stresses have a considerable effect on both the local and the member stability behaviour of steel structures is accepted, but it is still studied, improved and applied in practise and design [5]. The design buckling resistance $N_{b,Rd}$ of the compression members is predicted from formula [2]:

$$N_{b,Rd} = \frac{\chi A f_y}{\gamma_{M1}} \qquad (1)$$

where: $\chi$ – reduction factor for relevant buckling mode, $f_y$ – yield strength of steel, $A$ – cross-section area, $\gamma_{M1}$ – partial safety factor for instability.

The reduction factor $\chi$ is obtained from one of five buckling curves, created as a result of calibration based on experimental, analytical and numerical investigations. Such buckling curves are physically connected with type of cross-section, initial out-of-straightness, and magnitude of residual stresses due to the different manufacturing process. For steel angle sections, provisions [2] recommend the curve 'b', but the EN 50341-1 standard [6] allows one to choose the less conservative curve '$a_0$'. This discrepancy shows that the issue of determining the buckling resistance of angles subjected to compression remains a subject of further research.

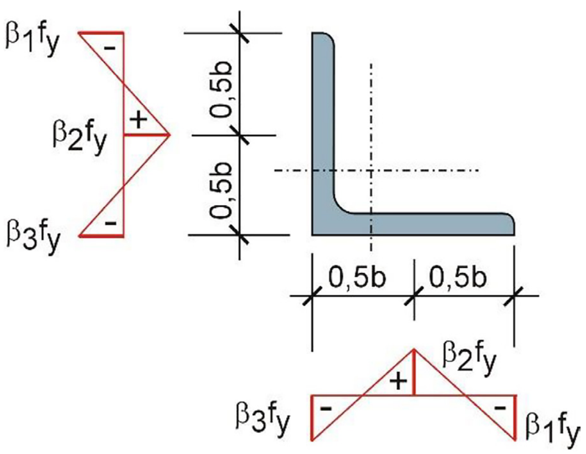


**Figure 1.** Residual stress distribution model of hot rolled steel angles

So far, the current design provisions do not take directly into account the impact of hot-dip galvanising process of an element on the reduction of residual stresses and thus the reduction of generalised imperfection in the Ayrton-Perry model. Hot-dip galvanising is now the basic method of protecting elements in steel masts and towers, especially those made of angle sections, against corrosion. Galvanising temperature has been reported to have little effect on the material strength and ductility, as higher temperatures are needed to produce metallurgical changes, but this process inevitably changes and relieves residual stress [7, 8]. The decrease in the magnitude of residual stresses reduces the extent of generalised imperfection and can improve member behaviours under axial compressive loads, which results in an increase in the buckling resistance of the element [9, 10].

The bilinear distributions of the residual stresses from hot rolling, obtained on the basis of various tests, are shown in Figure 1. The peak values of the residual stresses are related to the yield strength of the steel. Their values, assumed in the calibration of the buckling curves in the standards, are listed in Table 1.

The values of the residual stress factors shown in Table 1 include the effect of hot rolling. In the case of subsequent hot-dip galvanisation, heating the section to a temperature of 450 °C [14] and cooling to room temperature reduces these values. Recent experimental research reports that an average reduction in the peak values of the principal residual stress observed in the case of thin-walled steel sections is in the range of 47–60%, compared to the initial value [7, 9, 10].

The purpose of this paper is to assess the difference between the relative buckling resistance of compressed elements with residual stresses resulting from hot rolling and the relative buckling resistance of the same elements in which the magnitude of residual stresses was decreased by the hot-dip galvanising process to 50% of their initial values. Relative buckling resistance is described by reduction factor values $\chi$, which can be evaluated from Equation 1, as:

$$\chi = \frac{N_{b,Rd}\, \gamma_{M1}}{A f_y} \qquad (2)$$

For the purposes of experimental tests or numerical analyses, the design buckling resistance $N_{b,Rd}$ is determined as the ultimate load $N_{ult}$ of the element subjected to compression, the partial factor is not taken into account ($\gamma_{M1}$ = 1.0), and the

**Table 1.** Residual stress factors of bilinear models

| Source | Residual stress factors | | |
|---|---|---|---|
| | $\beta_1$ [-] | $\beta_2$ [-] | $\beta_3$ [-] |
| European provisions [3] | -0.22 | 0.24 | -0.25 |
| United States provisions [11, 12] | -0.30 | 0.30 | -0.30 |
| Może et al. [13] | -0.20 | 0.20 | -0.20 |

**Note:** the minus (-) and plus (+) sign correspond to the compressive and tensile residual stresses, respectively.

product of the cross-sectional area $A$ and the yield strength $f_y$ is equal to the plastic resistance of the cross-section $N_{pl}$, according to the mentioned Ayrton-Perry model, which gives the following relationship:

$$\chi = \frac{N_{ult}}{N_{pl}} \tag{3}$$

As a method of solving such an issue, geometrically and materially non-linear analysis with imperfections (GMNIA) was applied, with the use of finite element method. The GMNIA approach is now used as an effective tool to solve instability problems, both in global and local ranges [15–17].

In the first step, a numerical model of the steel angle column subjected to compression was built, covering imperfections, geometrical and material nonlinearities. Then, it was checked on the basis of the results of our own experimental tests, and after validation, in the third step, a parametric study of these elements was performed.

The analysis carried out allowed one to obtain buckling curves of steel equal leg angle sections L65 × 65 × 7, in which in one group there were residual stresses with magnitude resulting from the hot rolling process, and in the other group there were residual stresses that were reduced by the hot-dip galvanising process. The buckling curves obtained in this way were compared with the design provisions.

## COMPUTATIONAL MODEL – GMNIA ANALYSIS

### Geometry, elements, and boundary conditions

The finite element model was obtained by geometric discretization of the L65 × 65 × 7 angle section with the use of shell elements. A geometrical model was created based on the mid-surface of the member (Fig. 2a) and its nominal dimensions. The model was discretised to obtain a uniform mesh size of about 5 mm. Shell elements with four nodes were used, with six degrees of freedom per node.

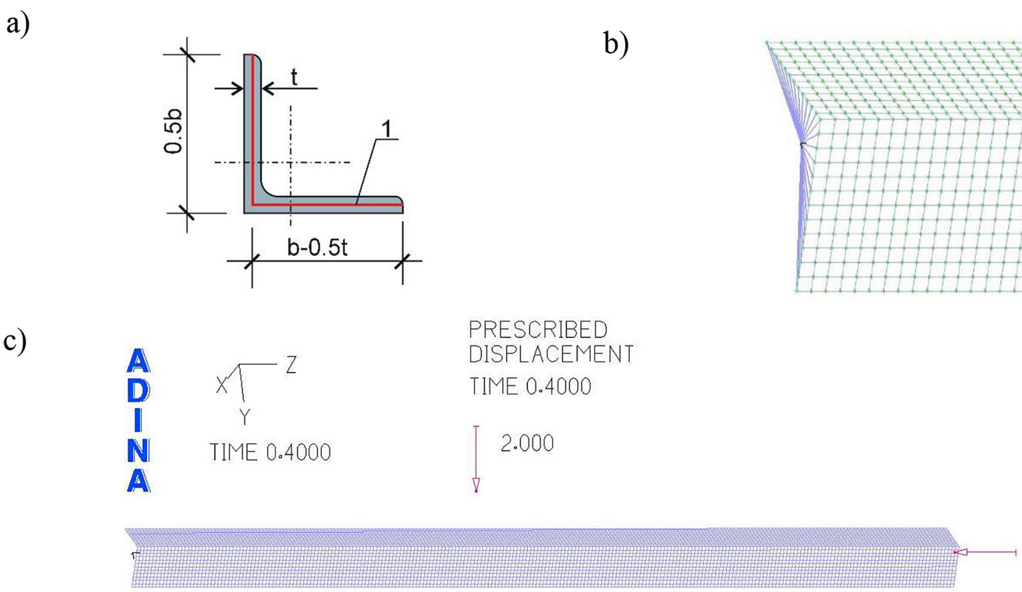


**Figure 2.** Geometry and support conditions of FE model: (a) cross-section and its mid-surface (1), (b) support conditions using rigid links, (c) FE model perspective

The lengths of the columns considered were equal to those used in the experiments performed or assumed in a parametric study (their dimensions are described in the following sections). Support conditions were modelled using rigid links between the column ends (lines along both angle legs) and an additional points lying in the centre of cross-section. Such a kinematic coupling enables the easy application of boundary conditions by assigning them to this additional point. In the validation case, the support conditions reproduced fixed end boundary conditions; in the case of parametric analysis, pin-end support was considered. In both cases, the initial load eccentricity was not considered.

The compression load was applied as the prescribed longitudinal displacement imposed on the top element, at an additional point in the centre of cross-section, to capture the post-buckling behaviour. The load was applied in about 20 steps until the ultimate load capacity was reached and then in a dozen or so steps in the post-critical phase. Figures 2b and 2c show geometry, mesh and support conditions used in models.

### Material model

Linear elastic – perfectly plastic material model with nominal plateau slope for numerical stability ($E_t = E / 10000$) was used, as recommended for steel grades exhibiting a sharply defined yield point and yield plateau. The yield point adopted in the numerical models was determined from the coupon test (see Table 3 in the next section) in the case of the validation phase, or as nominal values as for steel grade S355 in the case of parametric analysis.

### Geometrical imperfections

The initial geometric imperfection of a member (out-of-straightness) was introduced as the first buckling mode. Eigenmodes are accepted to represent the most dangerous forms of imperfections, and their introduction in that form is considered as the classical approach [18]. The shape of such an imperfection was obtained from linear bifurcation analysis (LBA). An imperfection amplitude prescribed to the point furthest from the initial straight axis was equal to the measured value in the validation phase, or equal to $L / 1000$ in the parametric analysis. The value of $L / 1000$ is consistent with the recommendations [3] and constitutes the limits of the manufacturing tolerances of elements with length $L$ from the straightness [19]. The first buckling modes calculated by the LBA analysis, in the case of a parametric study (with pin-end supports), is shown in Figure 3.

### Residual stress distribution

The bilinear residual stress distribution model shown in Figure 1 was adopted in the FE model (Fig. 4). Residual stress factors were assumed as $\beta_1 = -0.25$; $\beta_2 = 0.25$ and $\beta_3 = -0.25$ for hot rolled angles without subsequent hot-dip galvanisation and $\beta_1 = -0.125$; $\beta_2 = 0.125$ and $\beta_3 = -0.125$ for hot rolled and hot-dip galvanised angles. In the FE model, initial stresses were introduced as initial conditions using the geometry surface properties option. Each angle leg was divided into 12 longitudinal surfaces that ran throughout the length of the element. In each of such strips, finite elements have been assigned an appropriate value of normal stresses $\sigma_{zz}$, longitudinal to the axis of the element, resulting from the approximation of the residual stresses with a stepped distribution, Figure 4a. The distribution of residual stresses obtained in the FE model, after the equilibrium step, along the width of one angle leg, in the case of hot rolling only, is shown in Figure 4b, and the distribution of residual stresses in the case of subsequent hot-dip galvanising is shown in Figure 4c. Both cases concern elements made of S355

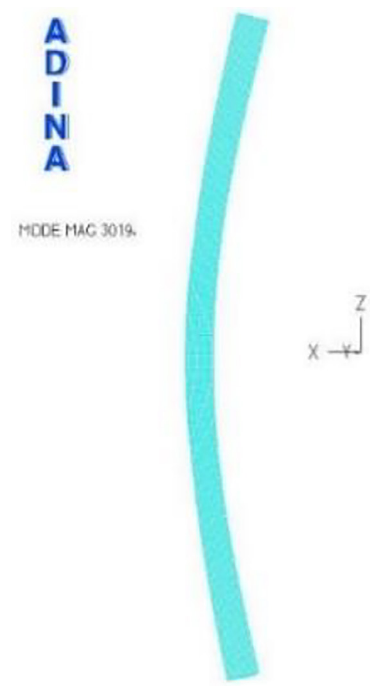


**Figure 3.** The first buckling mode considered as geometrical imperfection

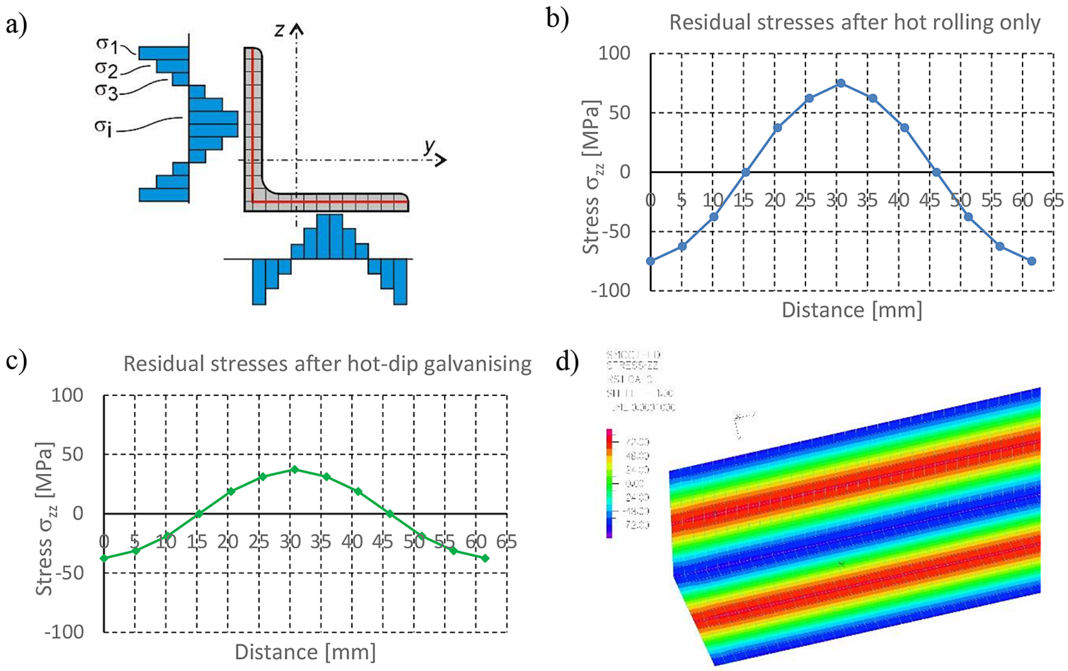


**Figure 4.** Residual stresses in the FE model: (a) approximation of residual stress, (b) distribution of residual stresses along the width of one angle leg in the case of hot rolling only, (c) distribution of residual stresses along the width of one angle leg in the case of hot-dip galvanising, d) perspective of residual stresses in FE model

steel grade (parametric analysis phase). Figure 4d also shows the distribution of residual stress in the two legs of angle. The variations in residual stress through thickness of the legs were omitted. The are reported to have no significant influence on the buckling resistance [9].

All numerical studies were performed with the help of ADINA finite element software [20]. Geometric non-linearity (large displacement) was introduced to take into account second-order effects, so the type of analysis applied was geometrically and materially non-linear analysis with imperfections (GMNIA).

## VALIDATION

### Experimental test

The own experimental study included three groups of specimens, made from single angles with length members equal to 1500, 1200 and 900 mm. A summary of all specimens is presented in Table 2. All specimens were hot-dip galvanised according to current industrial practice. The average thickness of the zinc coating was about 100 µm. The average mechanical steel properties of the specimens, based on the coupon test, are summarised in Table 3. The residual stress distribution and their values in the specimens were not measured.

The actual geometries of the cross-sectional dimensions of the specimens and the deviation of the axis from its ideal straight position were measured for each specimen. Imperfections along the length of the element were measured using a displacement transducer in selected cross sections, in the *y* and *z* directions (*dy* and *dz*), approximately at the height of the centre of gravity of the section, based on the datum line, Figure 5a. Then, on the basis of these measurements, the geometric imperfection was calculated, in the form of initial out-of-straightness in the *u* and *v* directions. An

**Table 2.** Details of the specimens

| Specimen group | Section | Length, [mm] | No. of tested elements |
|---|---|---|---|
| US-1500 | L65 × 65 × 7 | 1500 | 5 |
| US-1200 | L65 × 65 × 7 | 1200 | 5 |
| US-900 | L65 × 65 × 7 | 900 | 5 |

**Table 3.** Material properties

| Coupons | $f_{y,mean}$ [MPa] | $f_{u,mean}$ [MPa] | $\varepsilon_{u,mean}$ [-] |
|---|---|---|---|
| L65 × 65 × 7 | 302.1 | 419.6 | 0.176 |

example of real geometrical shapes of the tested specimens in group US-1500 are shown in Figures 5b and 5c.

The tests were carried out on an INSTRON 1200 kN J1D testing machine, which measured the applied load and also the shortening of the test element. All specimens were loaded monotonically until failure, by imposed displacement, which allowed the trace of post-buckling behaviour. The load increment rate was equal to 0.005 mm/min. The concentric compression force was introduced into the specimen. The specimens were fixed at both ends on the test rig – no rotation about the minor and major axes, and no twist or warping was possible.

The spatial form of the stability loss was observed in the tested specimens by measuring the lateral displacements of four markers located in the middle of the height of each specimen. Measurement of these displacements was carried out by the non-contact method, using the ARAMIS Adjustable 12 M digital image correlation system. The optical axis of the camera was set parallel to the axis of the test element ($x$-axis), and the observed displacements of markers' took place in a plane perpendicular to the axis of the rod [21]. From these readings, both the lateral displacements of the centre of gravity in the $u$ and $v$ directions, and also the torsion of the cross section $\varphi$ were calculated. The general view of the tested rig and the layout of the instrumentation are shown in Figure 6.

## Comparison of results between experimental tests and GMNIA

The comparison between the results obtained from the FE model and the experimental research showed that the numerical model correctly reproduces the physical phenomena, especially the failure modes observed during the tests, the ultimate load values, and the post-buckling behaviour. In both cases (FE modelling and experimental test), the failure mode was clearly flexural buckling about the $v$-$v$ axis. Model validation took place in the ultimate load domain. Table 4 shows the ultimate load values from the test $N_{ult,mean,test}$ (mean value of five specimens and their coefficients of variation), and also ultimate load value from FE modelling $N_{ult,FEM}$. It can be seen that comparison between these values shows quite good accuracy. The load-deformation curves for the S-1200 group (specimens with length L = 1200 mm), where displacement was measure in the middle height of specimen in the u direction, are also shown in Figure 7.

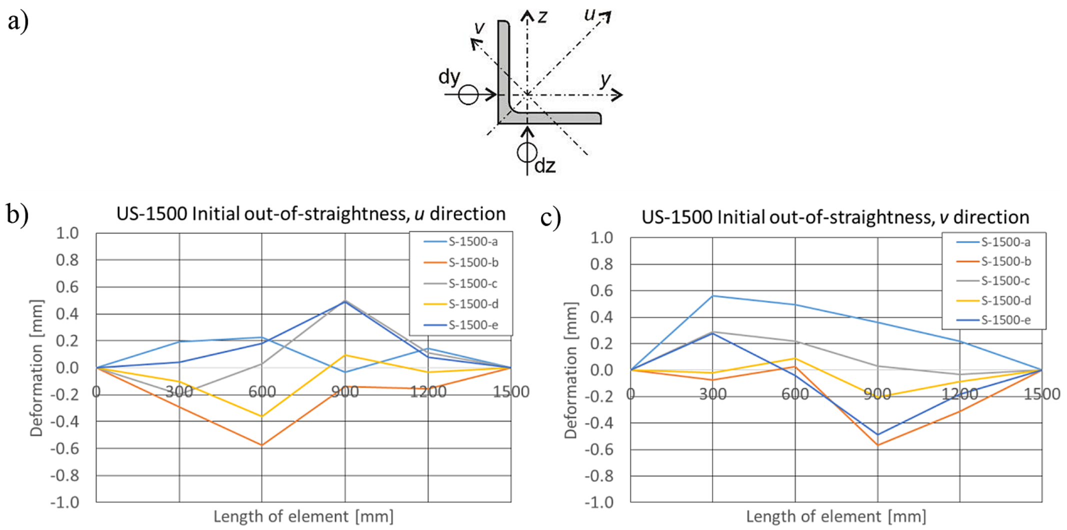


**Figure 5.** Measured initial geometric imperfection (out-of-straightness) of specimen US-1500; (a) method of measurement, (b) initial out-of-straightness in the $u$ direction, (c) initial out-of-straightness in the $v$ direction

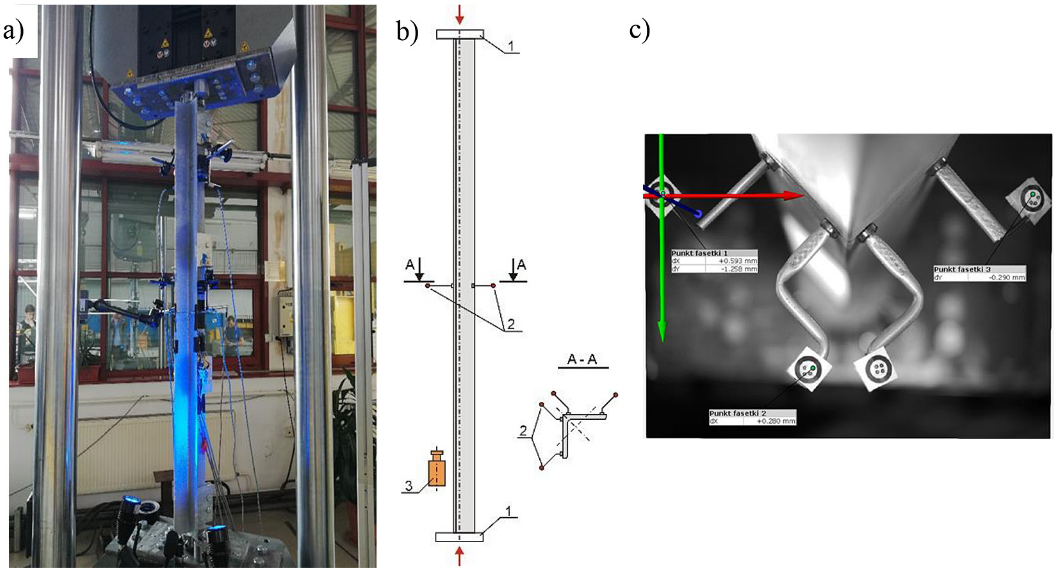


**Figure 6.** Experimental test; (a) general view of test rig, (b) layout of instrumentation, c) view of the camera on the markers (1 – support, 2 – markers for digital image correlation, 3 – ARAMIS system camera)

In creating the FE model, the actual (measured) deviations of the non-straightness of the longitudinal axis of the element were used (the assumed bow imperfection was equal to the largest measured value within the entire group, see Fig. 5) and the residual stresses distribution according to Figure 1, with values reduced due to the hot-dip galvanising process ($\beta_1$ = -0.125; $\beta_2$ = 0.125 and $\beta_3$ = -0.125). Also, the real yield strength of the steel from the coupon test (Table 3) was used to model the properties of the material.

## PARAMETRIC STUDY AND RESULTS

The experimental tests carried out allowed one to obtain only three values of the sought χ reduction factor. To expand the number of results obtained, a parametric study was performed using a calibrated FE model of the steel angle subjected to compression using GMNIA analysis. The aim of the study was to obtain the values of reduction factors χ in a wider range of slenderness of the angles considered and to directly compare the values of the reduction factors obtained when modelling a compressed bar having a full field of residual stresses, as after hot rolling, with one in which the residual stresses are reduced by the hot-dip galvanising process. It was used following assumptions:

- the lengths of the elements considered ranged from 380 mm to 2022 mm, covering the relative slenderness of the elements $\bar{\lambda}$ in the range between 0.4 and 2.10. The resulting parametric analysis plan is shown in Table 5,
- modelled elements have the cross-section dimension of the angle sections L65 × 65 × 7, and mechanical properties of steel grade S355,
- the imperfections were explicitly included and as geometrical out-of-straightness with equivalent bow equal to *L* / 1000 and with the effects of residual stresses. Two distributions of residual stresses were included in the analysis: the first with magnitude according to Fig. 1 and peak values described by factors $\beta_1$ = -0.25; $B_2$ = 0.25 and $\beta_3$ = -0.25 (for

**Table 4.** Ultimate load $N_{ult}$ from test and GMNIA analysis

| Specimens | Test results | | FEM analysis | Difference, [%] $\frac{N_{ult,FEM} - N_{ult,mean,test}}{N_{ult,mean,test}}$ |
|---|---|---|---|---|
| | Ultimate load $N_{ult,mean,test}$ [kN] | Coefficient of variation [%] | Ultimate load $N_{ult,FEM}$ [kN] | |
| US-1500 | 219.0 | 8.3 | 225,8 | 3.1 |
| US-1200 | 241.4 | 2.7 | 237,9 | -1.4 |
| US-900 | 249.9 | 0.9 | 255.7 | 2.3 |

**Note:** The ultimate load from test $N_{ult,mean,test}$ is an average value obtained from 5 specimens.

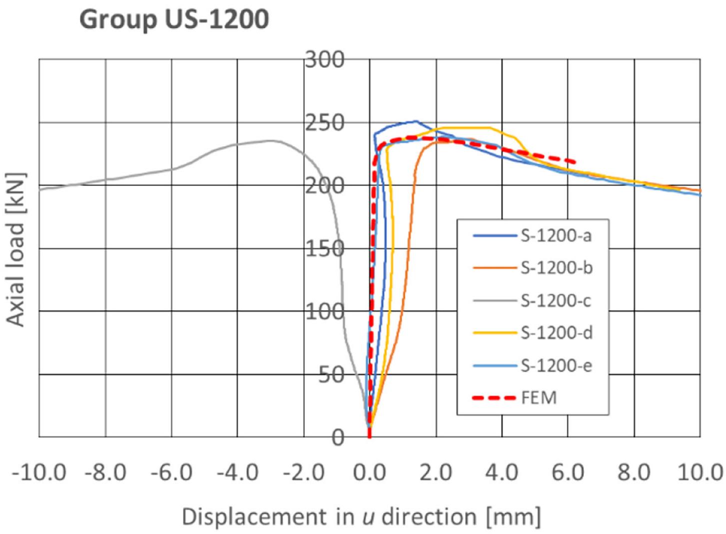


**Figure 7.** Load-displacement curves for the US-1200 group

hot-rolled angles), and the second with magnitude of residual stress halved due to subsequent hot-dip galvanisation $\beta_1$ = -0.125; $\beta_2$ = 0.125 and $\beta_3$ = -0.125.

All considered lengths of compressed angles were subjected to a double computational analysis. Once, by assigning a larger residual stress field (originating from hot rolling), and the second time, by reducing the residual stress field by half (according to the hot-dip galvanising process). In each case, force-displacement curves were obtained in which the highest value of the load force determined the ultimate load $N_{ult}$ of the angle. Based on the determined ultimate load $N_{ult}$, reduction factors were calculated from Equation 3. Reduction factors determined for elements with a residual stress field after hot rolling are marked with the symbol $\chi_{100\%}$, reduction factors for elements with a reduced residual stress field by half (effect of hot-dip galvanizing) are marked as $\chi_{50\%}$. Their values are listed in Table 5.

The dependence of the reduction factors determined in this way on the relative slenderness of the elements is shown in Figure 8, against the buckling curves ‘$a_0$’, ‘a’ and ‘b’ according to EN 1993-1-1 [2].

An increase in the relative buckling resistance of hot-dip galvanised elements can be seen in which the residual stress field has been decreased by this process. This increase ranges from 2 to 7%. The analyses confirmed that the reduction factors $\chi_{50\%}$ exhibit values closer to the buckling curve ‘a’, but these values do not reach the ‘$a_0$’ curve recommended by EN 50341-1 standard [6]. Experimental tests also do not show a clear possibility of using the buckling curve ‘$a_0$’ in the case of hot-dip galvanised angles instead of the curve ‘b’.

**Table 5.** The range of parametric study and reduction factors obtained

| Length of the column L [mm] | Slenderness $\lambda = L/i_v$ [-] | The relative slenderness $\bar{\lambda}$ [-] | Reduction factor $\chi_{100\%}$ [-] | Reduction factor $\chi_{50\%}$ [-] |
|---|---|---|---|---|
| 385 | 30.6 | 0.40 | 0.917 | 0.940 |
| 578 | 45.9 | 0.60 | 0.834 | 0.879 |
| 770 | 61.1 | 0.80 | 0.740 | 0.794 |
| 963 | 76.4 | 1.00 | 0.638 | 0.683 |
| 1155 | 91.7 | 1.20 | 0.523 | 0.548 |
| 1348 | 107.0 | 1.40 | 0.431 | 0.444 |
| 1540 | 122.2 | 1.60 | 0.337 | 0.345 |
| 1733 | 137.5 | 1.80 | 0.275 | 0.279 |
| 2022 | 160.5 | 2.10 | 0.202 | 0.206 |

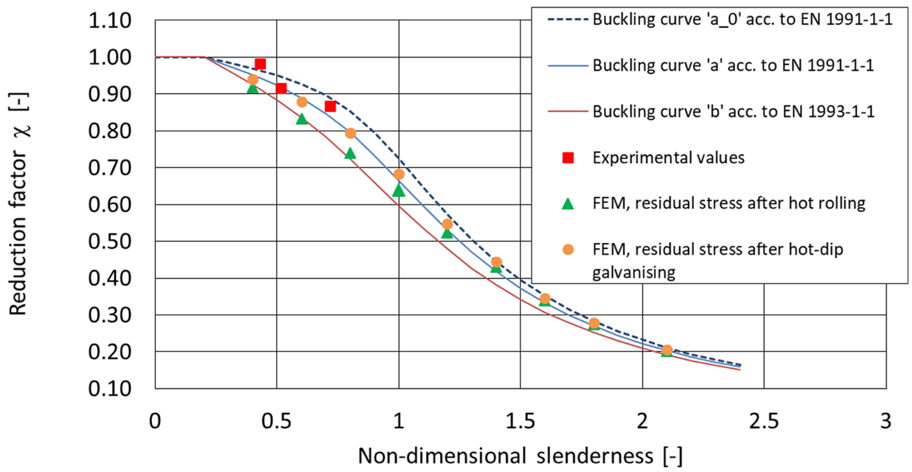


**Figure 8.** Obtained reduction factors against buckling curves ‘a’ and ‘b’

## CONCLUSIONS

Conducted research and numerical analyses showed that residual stresses in equal leg steel angles significantly influence their buckling resistance. Reliving of residual stresses by hot-dip galvanising process increases the value of reduction factor $\chi$, but it is a relatively small increase of 2 to 7% compared to elements with a residual stress field after hot rolling. The increase is greatest in the relative slenderness of the elements in the range of 0.6–1.0. GMNIA analyses have shown that the buckling curve suitable for angles with flexural buckling is the curve ‘b’. Hot-dip galvanising does not allow the assignment of angles to the buckling curve ‘$a_0$’ according to the EN 50341-1 [6]. Perhaps, an increase in buckling resistance of hot-dip galvanising elements could be taken into account in expert work and when assessing the load-bearing capacity of existing structures.

### Acknowledgements

The research leading to these results has received funding from the commissioned task entitled “VIA CARPATIA Universities of Technology Network named after the President of the Republic of Poland Lech Kaczyński” contract no. MEiN/2022/DPI/2575 action entitled “In the neighbourhood - inter-university research internships and study visits”.

## REFERENCES

1. Vayas I., Jaspart J.-P., Bureau A., Tibolt M., Reygner S., Papavasiliou M. Telecommunication and transmission lattice towers from angle sections – the ANGELHY project. ce/papers 2021; 4(2–4): 210–217. https://doi.org/10.1002/cepa.1283
2. EN 1993-1-1 Eurocode 3: Design of steel structures - Part 1-1: General rules and rules for buildings. CEN, 2005. Brussels.
3. ECCS. Manual on stability of steel structures. European Convention for Constructional Steelwork, 1976. http://www.eccspublications.eu
4. Augustyn J. The influence of residual (welding) stresses on the stability of compression elements (in Polish). Inżynieria i Budownictwo 1962; 10: 392–395.
5. Schaper L., Tankova T., da Silva L. S., Knobloch. M. Effects of state-of-the-art residual stress models on the member and local stability behaviour. Steel Construction, 2022; 15(4): 244–254. https://doi.org/10.1002/stco.202200027
6. EN 50341-1 Overhead electrical lines exceeding AC 1 kV - Part 1: General requirements - Common specifications. CEN, 2012, Brussels.
7. Jin Y., Sun M., Karimi K., Ziaeinejad A., Tayyebi K., Flores M. Effects of galvanizing on residual stresses and stress concentrations in RHS X-and T-Connections. Engineering Structures, 2013; 284: 115984. https://doi.org/10.1016/j.engstruct.2023.115984
8. Sun M., Packer J. A. Hot-dip galvanizing of cold-formed steel hollow sections: A state-of-the-art review. Front. Struct. Civ. Eng, 2019; 13(1): 49–65. https://doi.org/10.1007/s11709-017-0448-0
9. Chou A. P., Shi G., Liu C., Zhou L. Residual

stress and compression buckling of large welded equal-leg steel angles. Journal of Constructional Steel Research, 2023; 201, 107756. https://doi.org/10.1016/j.jcsr.2022.107756

10. Shi G., Zhang Z., Zhou L., Gao Y. Experimental study and modeling of residual stresses of Q420 large-section angles. Journal of Constructional Steel Research, 2020; 167, 105958. https://doi.org/10.1016/j.jcsr.2020.105958
11. Kitipornchai S., Lee H. W. Inelastic buckling of single-angle. tee and double-angle struts. Journal of Constructional Steel Research, 1986; 6(1): 3–20. https://doi.org/10.1016/0143-974X(86)90018-0
12. Kitipornchai S., Lee H. W. Inelastic experiments on angle and tee struts. Journal of Constructional Steel Research, 1986; 6(3), 219–236. https://doi.org/10.1016/0143-974X(86)90035-0
13. Može P., Cajot L. G., Sinur F., Rejec K., Beg. D. Residual stress distribution of large steel equal leg angles. Engineering Structures, 2014; 71: 35–47. https://doi.org/10.1016/j.jcsr.2022.107756
14. Kuklík V., Kudlacek J. Hot-dip galvanizing of steel structures. Butterworth-Heinemann, 2016.
15. de Menezes A.A., Vellasco P.C.D.S., de Lima L.R., da Silva A.T. Experimental and numerical investigation of austenitic stainless steel hot-rolled angles under compression. Journal of Constructional Steel Research, 2019; 152: 42–56, https://doi.org/10.1016/j.jcsr.2018.05.033
16. Shi G., Zhou W.J., Bai Y., Liu, Z. Local buckling of steel equal angle members with normal and high strengths. International Journal of Steel Structures, 2014; 14: 447–455. https://doi.org/10.1007/s13296-014-3002-0
17. Filipović A., Dobrić J., Marković Z., Baddoo N., Flajs Ž. Buckling resistance of stainless steel angle column. Građevinar, 2019; 71: 547–558. https://doi.org/10.14256/JCE.2563.2018
18. Rzeszut. K., Garstecki A. Modeling of initial geometrical imperfections in stability analysis of thin-walled structures. Journal of Theoretical and Applied Mechanics, 2009; 47(3): 667–684. http://ptmts.org.pl/jtam/index.php/jtam/article/view/v47n3p667
19. EN 1090-2 Execution of steel structures and aluminium structures - Part 2: Technical requirements for steel structures. CEN, 2018, Brussels.
20. ADINA 9.8. ADINA Theory and Modeling Guide Volume I: ADINA Solids & Structures. 2022.
21. Jastrzębski K., Ślęczka L. Strengthening of axially compressed bars in lattice towers under load–experimental investigations. ce/papers, 2023; 6(3–4): 1105–1110. https://doi.org/10.1002/cepa.2413